

## Effect of vector–axial-vector mixing to dilepton spectrum in hot and/or dense matter \*

Masayasu Harada

*Department of Physics, Nagoya University, Nagoya, 464-8602, JAPAN  
E-mail: harada@hken.phys.nagoya-u.ac.jp*

Chihiro Sasaki

*Frankfurt Institute for Advanced Studies, J.W. Goethe University, D-60438 Frankfurt, Germany  
Physik-Department, Technische Universität München, D-85747 Garching, Germany  
E-mail: sasaki@fias.uni-frankfurt.de*

In this write-up we summarize main results of our recent analyses on the mixing between transverse  $\rho$  and  $a_1$  mesons in hot and/or dense matter. We show that the axial-vector meson contributes significantly to the vector spectral function in hot matter through the mixing. In dense baryonic matter, we include a mixing through a set of  $\omega\rho a_1$ -type interactions. We show that a clear enhancement of the vector spectral function appears below  $\sqrt{s} = m_\rho$  for small three-momenta of the  $\rho$  meson, and thus the vector spectrum exhibits broadening.

### 1. Introduction

In-medium modifications of hadrons have been extensively explored in the context of chiral dynamics of QCD.<sup>3,4</sup> Due to an interaction with pions in the heat bath, the vector and axial-vector current correlators are mixed. At low temperatures or densities a low-energy theorem based on chiral symmetry describes this V-A mixing.<sup>5</sup> The effects to the thermal vector spectral function have been studied through the theorem,<sup>6</sup> or using chiral reduction formulas based on a virial expansion.<sup>7</sup>

In Ref. 1, it was shown that the effects of the V-A mixing, and how the axial-vector mesons affect the spectral function near the chiral phase transition, within an effective field theory. The analysis was carried out assuming several possible patterns of chiral symmetry restoration: dropping or non-dropping  $\rho$  meson mass along with changing  $a_1$  meson mass, both considered to be options from a phenomenological point of view.

In Ref. 2, we studied a novel effect of the V-A mixing through a set of  $\omega\rho a_1$ -type interactions at finite baryon density, which was introduced by a Chern-Simons term in a holographic QCD model.<sup>8</sup> We focused on the V-A mixing at tree level and its

---

\* Talk given by M. Harada at 2009 Nagoya Global COE Workshop “Strong Coupling Gauge Theories in LHC Era (SCGT09)”. This talk is based on the work done in Refs. 1,2

consequence on the in-medium spectral functions which are the main input to the experimental observables. We showed that the mixing produces a clear enhancement of the vector spectral function below  $\sqrt{s} = m_\rho$ , and that the vector spectral function is broadened due to the mixing. We also discussed its relevance to dilepton measurements.

In this write-up, we summarize main results of these papers especially focusing on the effect to the vector spectral function.

## 2. Effects of Vector–Axial-vector Mixing in Hot Matter

We start with showing the vector spectral function at  $T/T_c = 0.6$ , without any dropping masses, in Fig. 1 (left). Two cases are compared; one includes the V-A mixing and the other does not. Both the spectral functions has a peak at  $M_\rho$ . The effects of V-A mixing can be seen as a shoulder at  $\sqrt{s} = M_{a_1} - m_\pi$  and a bump above  $\sqrt{s} = M_{a_1} + m_\pi$ .

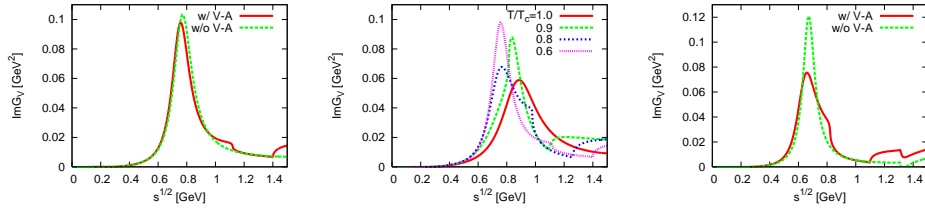


Fig. 1. Left figure shows the vector spectral function at temperature  $T/T_c = 0.6$ . The solid (red) curve includes the effect of V-A mixing, while the dashed (green) curve does not. The middle figure shows the spectral function (option (A)) for  $m_\pi = 140$  MeV at several temperatures  $T/T_c = 0.6-1.0$ . The right figure shows the vector spectral function (option (B)) for  $m_\pi = 140$  MeV in type (I) at temperature  $T/T_c = 0.8$ .

In Ref. 1, two possible cases of chiral symmetry restoration are studied:

- (A) Dropping  $a_1$  meson mass but non-dropping  $\rho$  mass;
- (B) Dropping  $\rho$  and  $a_1$  meson masses.

In both cases, the “flash temperature”<sup>9</sup>  $T_f$  is introduced for controlling how the mesons experience partial restoration of chiral symmetry. Then, the masses of vector and/or axial-vector mesons are assumed to have temperature dependences only above  $T_f$ . In option (A) at the chiral limit, the dropping  $a_1$  meson mass for  $T > T_f$  is taken as

$$\frac{M_{a_1}^2(T) - M_\rho^2}{M_{a_1}^2(T=0) - M_\rho^2} = \frac{T_c^2 - T^2}{T_c^2 - T_f^2}, \quad (1)$$

where  $T_c$  is the critical temperature of the chiral symmetry restoration. The vector spectral function for this option (A), with the effect of pion mass included, is shown at several temperatures in Fig. 1 (middle). Below  $T_c$  one observes the previously

mentioned threshold effects moving downward with increasing temperature. It is remarkable that at  $T_c$  the spectrum shows almost no traces of  $a_1$ - $\rho$ - $\pi$  threshold effects: The  $\rho$  to  $a_1$  mass ratio becomes almost 1 at  $T = T_c$  even though the effect of  $M_\pi$  is included. Furthermore, one can show that  $a_1$ - $\rho$ - $\pi$  coupling constant becomes very tiny,  $g_{a_1\rho\pi} \sim 0.06 m_\pi$ . This indicates that at  $T_c$  the  $a_1$  meson mass nearly equals the  $\rho$  meson mass and the  $a_1$ - $\rho$ - $\pi$  coupling almost vanishes even in the presence of explicit chiral symmetry breaking.

In option (B), two types of temperature dependences were used in Ref. 1:

$$(I) : \frac{M_\rho^2(T)}{M_\rho^2(T=0)} = \frac{T_c^2 - T^2}{T_c^2 - T_f^2}, \quad \frac{M_{a_1}^2(T) - M_\rho^2(T)}{M_{a_1}^2(T=0) - M_\rho^2(T=0)} = \left( \frac{T_c^2 - T^2}{T_c^2 - T_f^2} \right)^2, \quad (2)$$

$$(II) : \frac{M_\rho^2(T)}{M_\rho^2(T=0)} = \left( \frac{T_c^2 - T^2}{T_c^2 - T_f^2} \right)^2, \quad \frac{M_{a_1}^2(T) - M_\rho^2(T)}{M_{a_1}^2(T=0) - M_\rho^2(T=0)} = \frac{T_c^2 - T^2}{T_c^2 - T_f^2}. \quad (3)$$

Figure 1 (right) shows the vector spectrum using the type (I) parameterization at  $T = 0.8 T_c$ . The feature that the  $a_1$  meson suppresses the vector spectral function through the V-A mixing remains unchanged. Compared with the curve for  $T/T_c = 0.8$  in Fig. 1 (middle), a bump through the V-A mixing and the  $\rho$  peak are shifted downward since both the  $\rho$  and  $a_1$  masses drop. The self-energy has a cusp at the threshold  $2 M_\rho$  and this appears as a dip at  $\sqrt{s} \sim 1.3$  GeV. The influence of finite  $m_\pi$  turns out to be in threshold effects as before. We find that the nearly vanishing V-A mixing as seen for the non-dropping  $\rho$  mass, option (A).

The result given here shows that the axial-vector meson contributes significantly to the vector spectral function; the presence of the  $a_1$  reduces the vector spectrum around  $M_\rho$  and enhances it around  $M_{a_1}$ . A major change with both dropping  $\rho$  and  $a_1$  masses is a systematic downward shift of the vector spectrum. We observe that the  $a_1$ - $\rho$ - $\pi$  coupling almost vanishes at the critical temperature  $T_c$  and thus the V-A mixing becomes very tiny.

### 3. Effects of Vector–Axial-vector Mixing in Dense Matter

In this section, we summarize main points shown in Ref. 2.

At finite baryon density a system preserves parity but violates charge conjugation invariance. Chiral Lagrangians thus in general build in the term

$$\mathcal{L}_{\rho a_1} = 2C \epsilon^{0\nu\lambda\sigma} \text{tr} [\partial_\nu V_\lambda \cdot A_\sigma + \partial_\nu A_\lambda \cdot V_\sigma], \quad (4)$$

for the vector  $V^\mu$  and axial-vector  $A^\mu$  mesons with the total anti-symmetric tensor  $\epsilon^{0123} = 1$  and a parameter  $C$ . This mixing results in the dispersion relation<sup>8</sup>

$$p_0^2 - \bar{p}^2 = \frac{1}{2} \left[ m_\rho^2 + m_{a_1}^2 \pm \sqrt{(m_{a_1}^2 - m_\rho^2)^2 + 16C^2 \bar{p}^2} \right], \quad (5)$$

which describes the propagation of a mixture of the transverse  $\rho$  and  $a_1$  mesons with non-vanishing three-momentum  $|\vec{p}| = \bar{p}$ . The longitudinal polarizations, on the other hand, follow the standard dispersion relation,  $p_0^2 - \bar{p}^2 = m_{\rho, a_1}^2$ . When

the mixing vanishes as  $\bar{p} \rightarrow 0$ , Eq. (5) with lower sign provides  $p_0 = m_\rho$  and it with upper sign does  $p_0 = m_{a_1}$ . In the following, we call the mode following the dispersion relation with the lower sign in Eq. (5) “the  $\rho$  meson”, and that with the upper sign “the  $a_1$  meson”.

The mixing strength  $C$  in Eq. (4) can be estimated assuming the  $\omega$ -dominance in the following way: The gauged Wess-Zumino-Witten terms in an effective chiral Lagrangian include the  $\omega$ - $\rho$ - $a_1$  term<sup>10</sup> which leads to the following mixing term

$$\mathcal{L}_{\omega\rho a_1} = g_{\omega\rho a_1} \langle \omega_0 \rangle \epsilon^{0\nu\lambda\sigma} \text{tr} [\partial_\nu V_\lambda \cdot A_\sigma + \partial_\nu A_\lambda \cdot V_\sigma], \quad (6)$$

where the  $\omega$  field is replaced with its expectation value given by  $\langle \omega_0 \rangle = g_{\omega NN} \cdot n_B / m_\omega^2$ . One finds with empirical numbers  $C = g_{\omega\rho a_1} \langle \omega_0 \rangle \simeq 0.1$  GeV at normal nuclear matter density. As we will show below, this is too small to have an importance in the correlation functions. In a holographic QCD approach, on the other hand, the effects from an infinite tower of the  $\omega$ -type vector mesons are summed up to give  $C \simeq 1$  GeV  $\cdot (n_B/n_0)$  with normal nuclear matter density  $n_0 = 0.16$  fm<sup>-3</sup>.<sup>8</sup> In the following we assume an actual value of  $C$  in QCD in the range  $0.1 < C < 1$  GeV. Some importance of the higher Kaluza-Klein (KK) modes *even in vacuum* in the context of holographic QCD can be seen in the pion electromagnetic form factor at the photon on-shell: This is saturated by the lowest four vector mesons in a top-down holographic QCD model.<sup>11,12</sup> In hot and dense environment those higher members get modified and the masses might be somewhat decreasing evidenced in an in-medium holographic model.<sup>13</sup> This might provide a strong V-A mixing  $C > 0.1$  GeV in three-color QCD and the dilepton measurements may give a good testing ground.

In Fig. 2, we show the dispersion relations (5) for the transverse modes together with those for the longitudinal modes with  $C = 1$  and  $0.5$  GeV. This shows that, when  $C = 0.5$  GeV, there are only small changes for both  $\rho$  and  $a_1$  mesons, while a substantial change for  $\rho$  meson when  $C = 1$  GeV. For very large  $\bar{p}$  the longitudinal and transverse dispersions are in parallel with a finite gap,  $\pm C$ .

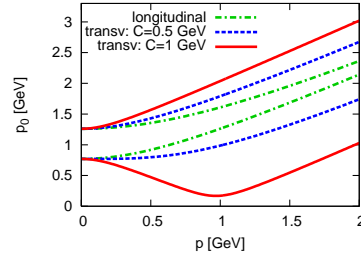


Fig. 2. The dispersion relations for the  $\rho$  (lower 3 curves) and  $a_1$  (upper 3 curves) mesons for  $C = 0.5$ , and  $1$  GeV.

In Fig. 3, we plot the integrated spectrum over three momentum, which is a main ingredient in dilepton production rates. Figure 3 (left) shows a clear enhancement of the spectrum below  $\sqrt{s} = m_\rho$  due to the mixing. This enhancement becomes much suppressed when the  $\rho$  meson is moving with a large three-momentum as shown in Fig. 3 (right). The upper bump now emerges more remarkably and becomes a clear indication of the in-medium effect from the  $a_1$  via the mixing.

As an application of the above in-medium spectrum, we calculate the production

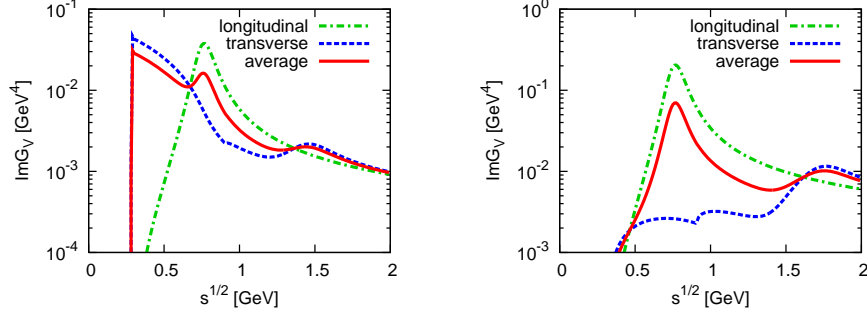


Fig. 3. The vector spectral function for  $C = 1$  GeV. The curves of the left figure are calculated integrating over  $0 < \bar{p} < 0.5$  GeV, and those of the right figure over  $0.5 < \bar{p} < 1$  GeV. Here we use the values of masses given by  $m_\pi = 0.14$  GeV,  $m_\rho = 0.77$  GeV,  $m_{a_1} = 1.26$  GeV, and the widths given by the imaginary part of one-loop diagrams in a chiral Lagrangian approach as<sup>2,14</sup> with the on-shell values of  $\Gamma_\rho(s = m_\rho^2) = 0.15$  GeV and  $\Gamma_{a_1}(s = m_{a_1}^2) = 0.33$  GeV.

rate of a lepton pair emitted from dense matter through a decaying virtual photon. Figure 4 (left) presents the integrated rate at  $T = 0.1$  GeV for  $C = 1$  GeV. One

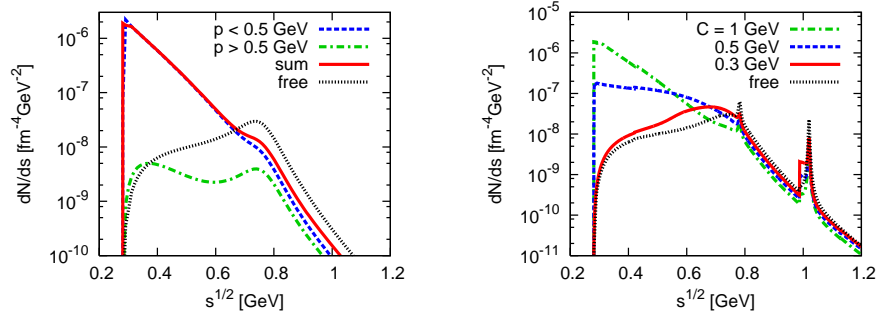


Fig. 4. Left figure shows the dilepton production rate at  $T = 0.1$  GeV for  $C = 1$  GeV. Integration over  $0 < \bar{p} < 0.5$  GeV (dashed) and  $0.5 < \bar{p} < 1$  GeV (dashed-dotted) was carried out. The right figure shows the dilepton production rate at  $T = 0.1$  GeV with various mixing strength  $C$ . Integration over  $0 < \bar{p} < 1$  GeV was done. We use the constant widths with values of  $\Gamma_\omega = 8.49$  MeV,  $\Gamma_\phi = 4.26$  MeV,  $\Gamma_{f_1(1285)} = 24.3$  MeV and  $\Gamma_{f_1(1420)} = 54.9$  MeV.

clearly observes a strong three-momentum dependence and an enhancement below  $\sqrt{s} = m_\rho$  due to the Bose distribution function which result in a strong spectral broadening. The total rate is mostly governed by the spectrum with low momenta  $\bar{p} < 0.5$  GeV due to the large mixing parameter  $C$ . When density is decreased, the mixing effect gets irrelevant and consequently in-medium effect in low  $\sqrt{s}$  region is reduced in compared with that at higher density. The calculation performed in hadronic many-body theory in fact shows that the  $\rho$  spectral function with a low momentum carries details of medium modifications.<sup>15</sup> One may have a chance to

observe it in heavy-ion collisions with certain low-momentum binning at J-PARC, GSI/FAIR and RHIC low-energy running.

It is straightforward to introduce other V-A mixing between  $\omega$ - $f_1(1285)$  and  $\phi$ - $f_1(1420)$ . In Fig. 4 (right) we plot the integrated rate at  $T = 0.1$  GeV with several mixing strength  $C$  which are phenomenological option. One observes that the enhancement below  $m_\rho$  is suppressed with decreasing mixing strength. This forms into a broad bump in low  $\sqrt{s}$  region and its maximum moves toward  $m_\rho$ . Similarly, some contributions are seen just below  $m_\phi$ . This effect starts at threshold  $\sqrt{s} = 2m_K$ . Self-consistent calculations of the spectrum in dense medium will provide a smooth change and this eventually makes the  $\phi$  meson peak somewhat broadened.

Finally, we remark that the importance of the mixing effect studied here relies on the coupling strength  $C$ . Holographic QCD predicts an extremely strong mixing  $C \sim 1$  GeV at  $n_B = n_0$  which leads to vector meson condensation at  $n_B \sim 1.1 n_0$ .<sup>8</sup> This may be excluded by known properties of nuclear matter and therefore in reality the strength  $C$  will be smaller. We have discussed a possible range of  $C$  to be  $0.1 < C < 1$  GeV based on higher excitations and their in-medium modifications. The parameter  $C$  does carry an unknown density dependence. This will be determined in an elaborated treatment of hadronic matter along with the underlying QCD dynamics. If  $C \sim 0.1$  GeV at  $n_0$  were preferred as the lowest-omega dominance, the mixing effect is irrelevant there. However, it becomes more important at higher densities, e.g.  $C = 0.3$  GeV at  $n_B/n_0 = 3$  which leads to a distinct modification from the spectrum in free space.

#### 4. Summary

In this write-up, we summarized main results of our recent analyses on the mixing between  $\rho$  and  $a_1$  mesons in hot and/or dense matter.

The analysis in Ref. 1 shows that the axial-vector meson contributes significantly to the vector spectral function in hot matter through the mixing: the presence of the  $a_1$  reduces the vector spectrum around  $M_\rho$  and enhances it around  $M_{a_1}$ . The effect of dropping mass of  $a_1$  with or without dropping  $\rho$  mass associated with the chiral symmetry restoration is studied. It is shown that the  $a_1$ - $\rho$ - $\pi$  coupling almost vanishes at the critical temperature  $T_c$  and thus the V-A mixing becomes very tiny.

In Ref. 2, we studied a novel effect of the V-A mixing through a set of  $\omega\rho a_1$ -type interactions at finite baryon density. We showed that the mixing produces a clear enhancement of the vector spectral function below  $\sqrt{s} = m_\rho$ , and that the vector spectral function is broadened due to the mixing.

It is an interesting issue to address a change of the vector correlator with the V-A mixing at finite baryon density in section 3 toward chiral symmetry restoration. The mixing (4) is chirally symmetric and thus does not vanish at the chiral restoration in contrast to the vanishing V-A mixing near the critical temperature  $T_c$  without baryon density in section 2. A spontaneous breaking of Lorentz invariance via the omega condensation could increase the mixing strength  $C$  near chiral

restoration.<sup>16</sup> Furthermore, if meson masses drop due to partial restoration of chiral symmetry assuming a second- or weak first-order transition in high baryon density but low temperature region, the ground state near the critical point may favor vector condensation even for a moderate mixing strength. This will be reported elsewhere.

### Acknowledgment

The work of M.H. is supported in part by the JSPS Grant-in-Aid for Scientific Research (c) 20540262, Grant-in-Aid for Scientific Research on Innovative Areas (No. 2104) “Quest on New Hadrons with Variety of Flavors” from MEXT and the Global COE Program of Nagoya University “Quest for Fundamental Principles in the Universe (QFPU)” from JSPS and MEXT of Japan. The work of C.S. is supported in part by the DFG cluster of excellence “Origin and Structure of the Universe”.

### References

1. C. Sasaki, M. Harada and W. Weise, *Prog. Theor. Phys. Suppl.* **174**, 173 (2008); *Phys. Rev. D* **78**, 114003 (2008); *Nucl. Phys. A* **827**, 350C (2009).
2. M. Harada and C. Sasaki, *Phys. Rev. C* **80**, 054912 (2009).
3. See, e.g., V. Bernard and U. G. Meissner, *Nucl. Phys. A* **489**, 647 (1988); T. Hatsuda and T. Kunihiro, *Phys. Rept.* **247**, 221 (1994); R. D. Pisarski, hep-ph/9503330; G. E. Brown and M. Rho, *Phys. Rept.* **269**, 333 (1996); F. Klingl, N. Kaiser and W. Weise, *Nucl. Phys. A* **624**, 527 (1997); F. Wilczek, hep-ph/0003183; G. E. Brown and M. Rho, *Phys. Rept.* **363**, 85 (2002).
4. R. Rapp and J. Wambach, *Adv. Nucl. Phys.* **25**, 1 (2000), R. S. Hayano and T. Hatsuda, arXiv:0812.1702 [nucl-ex], R. Rapp, J. Wambach and H. van Hees, arXiv:0901.3289 [hep-ph].
5. M. Dey, V. L. Eletsky and B. L. Ioffe, *Phys. Lett. B* **252**, 620 (1990), B. Krippa, *Phys. Lett. B* **427**, 13 (1998).
6. E. Marco, R. Hofmann and W. Weise, *Phys. Lett. B* **530**, 88 (2002), M. Urban, M. Buballa and J. Wambach, *Phys. Rev. Lett.* **88**, 042002 (2002).
7. J. V. Steele, H. Yamagishi and I. Zahed, *Phys. Lett. B* **384**, 255 (1996); *Phys. Rev. D* **56**, 5605 (1997), K. Dusling, D. Teaney and I. Zahed, *Phys. Rev. C* **75**, 024908 (2007), K. Dusling and I. Zahed, *Nucl. Phys. A* **825**, 212 (2009).
8. S. K. Domokos and J. A. Harvey, *Phys. Rev. Lett.* **99**, 141602 (2007).
9. G. E. Brown, C. H. Lee and M. Rho, *Nucl. Phys. A* **747**, 530 (2005).
10. N. Kaiser and U. G. Meissner, *Nucl. Phys. A* **519**, 671 (1990).
11. T. Sakai and S. Sugimoto, *Prog. Theor. Phys.* **113**, 843 (2005); *Prog. Theor. Phys.* **114**, 1083 (2005).
12. M. Harada, S. Matsuzaki and K. Yamawaki, in preparation. See also the contribution to the same proceedings.
13. K. Peeters, J. Sonnenschein and M. Zamaklar, *Phys. Rev. D* **74**, 106008 (2006).
14. M. Harada and C. Sasaki, *Phys. Rev. D* **73**, 036001 (2006).
15. F. Riek, R. Rapp, T. S. Lee and Y. Oh, *Phys. Lett. B* **677**, 116 (2009).
16. K. Langfeld, H. Reinhardt and M. Rho, *Nucl. Phys. A* **622**, 620 (1997), K. Langfeld and M. Rho, *Nucl. Phys. A* **660**, 475 (1999).